OPEN

Three-dimensional path of the body centre of mass during walking in children: an index of neural maturation

Chiara Malloggi[a], Viviana Rota[a], Luigi Catino[b], Calogero Malfitano[a], Stefano Scarano[a], Davide Soranna[c], Antonella Zambon[d] and Luigi Tesio[a,b,]

Few studies have investigated the kinematic aspects of the body centre of mass motion, that is, its three-dimensional path during strides and their changes with child development. This study aimed to describe the three-dimensional path of the centre of mass in children while walking in order to disentangle the effect of age from that of absolute forward speed and body size and to define preliminary pediatric normative values. The three-dimensional path of the centre of mass during walking was compared across healthy children 5–6—years (*n*=6), 7–8 years (*n*=6), 9–10 years (*n*=5), and 11–13 years of age (*n*=5) and healthy adults (23–48 years, *n*=6). Participants walked on a force-sensing treadmill at various speeds, and height normalization of speed was conducted with the dimensionless Froude number. The total length and maximal lateral, vertical, and forward displacements of the centre of mass path were calculated from the ground reaction forces during complete strides and were scaled to the participant's height. The centre of mass path showed a curved figure-of-eight shape. Once adjusted for speed and participants' height, as age increased, there was a decrease in the three-dimensional parameters and in the lateral displacement, with values approaching those of adults. At each step, lateral redirection of the centre of mass requires brisk transient muscle power output. The base of support becomes relatively narrower with increasing age. Skilled shortening of the lateral displacement of the centre of mass may therefore decrease the risk of falling sideways. The three-dimensional path of the centre of mass may represent maturation of neural control of gait during growth. *International Journal of Rehabilitation Research* 42: 112–119 Copyright © 2019 The Author(s). Published by Wolters Kluwer Health, Inc.

International Journal of Rehabilitation Research 2019, **42:**112–119

Keywords: children, maturation, neural control, three-dimensional path of centre of mass, walking

[a]Department of Neurorehabilitation Sciences, Istituto Auxologico Italiano, IRCCS, Ospedale San Luca, Milan, [b]Department of Biomedical Sciences for Health, Università degli Studi di Milano, Milan, [c]Scientific Direction, Istituto Auxologico Italiano, IRCCS, Milan and [d]Department of Statistics and Quantitative Methods, Università di Milano-Bicocca, Milan, Italy

Correspondence to Luigi Tesio, M.D., Dipartimento di Scienze Neuroriabilitative, Istituto Auxologico Italiano, IRCCS, Ospedale San Luca, via Mercalli 30, 20122 Milan, Italy
Tel: +39 2 58218150; fax: +39 2 58218155
e-mail: luigi.tesio@unimi.it; l.tesio@auxologico.it

Received 18 January 2019 **Accepted** 1 March 2019

Introduction

The motion of the body centre of mass (CoM) during locomotion represents a summary indicator of the motion of the whole body system (Cavagna, 2017). In recent decades, a study of the CoM motion has provided information on the mechanics of walking, both in humans and other animals, in terms of energy expenditure, mechanical efficiency, and symmetry between subsequent steps (Tesio *et al.*, 1998a). An 'inverted pendulum'-like mechanism, allowing a remarkable saving of muscular work, has been demonstrated in human adults (Tesio *et al.*, 1998a), children (Cavagna *et al.*, 1983), and biped and quadruped animals (Cavagna, 2017), as well as in adults (Tesio *et al.*, 1998b) and children (Bennett *et al.*, 2005) with various gait impairments.

Several studies have investigated energy changes associated with the CoM motion, but much less attention has been paid to kinematic aspects, that is, its three-dimensional (3D) path during strides. This has only been investigated in two studies of healthy adults (Tesio et al., 2010, 2011) and in one study of children (Dierick *et al.*, 2004). A key issue, still poorly understood, is the change in the 3D path of the CoM with a child's development. The development of mature walking reflects not only changes in body size and mass distribution (Jensen, 1989) but also maturation of the central nervous system. However, the staging of this usual process of development remains controversial.

Adult-like motion patterns are gradually observed between 4 and 13 years of age, with differences observed among papers and on the gait parameters considered. This holds for lower limb joint rotations (Sutherland *et al.*, 1980), lower limb electromyography patterns (Agostini *et al.*, 2010), and the power at the lower limb joints (Cupp *et al.*, 1999), etc. In contrast, the efficiency of the pendulum-like mechanical energy transfer of the CoM appears to be matured by age 5 years (Cavagna *et al.*, 1983; Dierick *et al.*, 2004). However, whether this also holds for

 DOI: 10.1097/MRR.0000000000000345

the 3D path of the CoM during a stride is unknown. In adults, once the forward average speed is controlled for, the 3D path appears to reflect a closed figure-of-eight shape that is upward concave on the frontal plane, which has been named the 'bow tie' (Tesio *et al.*, 2010), with an overall length in the order of 16–20 cm. Moreover, the path length and shape changes as a function of walking speed.

In the present study, the 3D path of the CoM during walking was analyzed in healthy children 5–13 years of age. The study aims were to disentangle the effect of age from that of absolute forward speed and body size and to define preliminary pediatric normative values. If these goals are met, the 3D path of the CoM during walking might present a possible index of the maturation of neural control of gait.

Participants and methods

Participants

Data were obtained from two previous studies (Tesio *et al.*, 2010, 2017). Data were analyzed from 22 healthy children (12 boys and 10 girls, 5–13 years of age) and six healthy adults (3 men and 3 women, 23–48 years of age, randomly selected from an original sample of 18). An even distribution across four age groups of children was as follows: 5–6 years ($n=6$); 7–8 years ($n=6$); 9–10 years ($n=5$); and 11–13 years ($n=5$).

Ethical considerations

Parental consent and child assent were obtained before participation in the study. Both children parents and adult participants gave written informed consent to the research and to the publication of the results. The experiments were conducted according to the Declaration of Helsinki of the World Medical Association, and the study protocol was approved by the local ethics committee.

Equipment

Participants walked on a split-belt treadmill (1.26 m long × 0.3 m wide for each independent half-treadmill; ADAL 3D; Medical-Development, Andrézieux-Bouthéon, France). Each half-treadmill was mounted on four piezoelectric force sensors (KI 9048B; Kistler, Winterthur, Switzerland) to record the 3D components of ground reaction forces during walking (Tesio *et al.*, 2017). Speed could be regulated in 0.1 m/s steps. In this study, force and speed signals were sampled at 250 Hz. The two half-treadmills ran at the same speed and force signals from both sides were summed vectorially, thus reproducing the signals generated from a single treadmill.

Experimental protocol

Participants wore a t-shirt, shorts, and light gym shoes. Height and weight were recorded (scale accuracy: 2 mm and 50 g, respectively). Spontaneous walking speed was calculated from an average of four 10-m-long trials in alternating directions along a 20-m corridor. Subsequently, participants were requested to stand quietly on the treadmill for about 6 s to obtain the vertical force calibration based on their weight. Then, they were allowed to adapt to walking on the treadmill for about 30 s.

During the experimental trial, participants were asked to walk for at least 45 s at different average speeds. These were increased in 0.1 m/s increments, up to each individual's spontaneous walking speed, or to the nearest attainable speed. Six subsequent strides with no visible changes in speed or any episodes of stumbling or imbalance were analyzed. The experimental conditions provided high reproducibility of results, thanks to the known and constant speed imposed by the treadmill (Tesio *et al.*, 2017). Participants were warned before each speed change, which took 5 s in a ramp-like fashion. Children were asked to look at a black spot (8 cm diameter) placed approximately at 2 m distance and at eye height on a white wall in front of the treadmill. For safety, a researcher provided a hand to the participant during speed-increasing phases to enable safe adaptation to the new walking condition. Children's parents or another relative also attended the session.

Computation of CoM 3D displacements

The 3D accelerations of the CoM were computed from the lateral (x), vertical (y), and forward (z) components of the resulting ground reaction force signals recorded during participants' walking for at least two entire steps on the force platforms. The 3D displacement and length of the CoM path were calculated on the basis of the so-called 'double-integration' or 'Newtonian' algorithms (from accelerations to speed and displacements) first proposed by Cavagna (1975). Participants' weights were subtracted from the vertical forces. Air and within-body frictions were neglected. The average vertical and lateral speed over the selected strides had to be nil and constant, and the same held for the forward speed, net of the average treadmill speed. To ensure these assumptions were met, there had to be no substantial drift in the average speeds of the CoM (Tesio *et al.*, 2017). For each selected stride, the maximal amplitude of lateral, vertical, and forward CoM displacements, and the total length of the CoM path, were calculated.

Normalization of the CoM 3D path

The maximal displacements in the x, y, and z directions, and the total length of the 3D path of the CoM, were normalized with respect to participants' height. The walking speed was normalized with the dimensionless Froude (Fr) number. The Fr number allows comparisons across individuals of different overall sizes but similar shapes in movements mostly constrained by gravity and inertia. In essence, it normalizes moments of inertia generated by the movements of different body segments (Alexander and Jayes, 1983; Cavagna *et al.*, 1983). The Fr number is computed according to the following equation:

$$Fr = \frac{V_f^2}{gh} \quad (1)$$

where V_f is the average treadmill speed, g the gravity acceleration, and h the participant's height. Fr normalization assigned different dynamically equivalent speeds to each individual, even when participants shared the same absolute forward speed. For walking, in Eq. (1) either height (as in the present study) or leg length can be used (Alexander and Jayes, 1983). Essentially, these are only proxies of the height of the CoM, expressed as a percentage of the total body height, which is influenced by the mass distribution within the body. However, in standing children (Swearingen and Young, 1965) and adults (Virmavirta and Isolehto, 2014), the location of the CoM lies at an invariant percentage (about 57%) of the participant's height. Stride periods were normalized to 100 time points.

Representation of the CoM path

Force and force-derived signals were synchronized and analyzed offline with algorithms available within the SMART Software Suite (BTS Bioengineering Spa, Milan, Italy). Stride period (one stride equals two consecutive steps) was defined as the time interval between three subsequent peaks of forward speed of the CoM following the heel strike. For graphic representation of the CoM path, results were averaged across six subsequent strides within each participant and then grand-averaged across each age group. Given that vertical, lateral, and forward (net of the treadmill) speeds are nil, the CoM path can be represented as a cyclic and closed 3D displacement around an average position (Fig. 1). Changes as a function of time were computed and analyzed as described in the next section.

Statistics

Continuous variables were expressed as means and SDs, while categorical data were expressed as frequencies. The effect of age group and Fr on each spatial parameter was evaluated with linear regression models with repeated measures. In these models, the within-subjects effects were 'walking speed' and 'step number' (Moser, 2004), and the fixed effects were 'age group' and 'Fr'. Moreover, to allow for a nonlinear relationship between Fr and each spatial parameter, a flexible regression modelling approach based on first-order and second-order fractional polynomials was applied (Royston *et al.*, 1999). In brief, for a regression model involving a single continuous covariate x, first- and second-order fractional polynomial models can be written as follows:

$$\text{First-order:} B_0 + B_1 \times x^p \quad (2)$$

$$\text{Second-order: } B_0 + B_1 \times x^p + B_2 \times x^q \quad (3)$$

Values of p and q are typically restricted to the set S € {−2, −1, −0.5, 0, 0.5, 1, 2, 3}, which provides practical flexibility. By convention, $x^0 = \log(x)$ and when $p = q$ then x^q is set to $x^p \times \log(x)$. The best functional form was then selected on the basis of Akaike's Information Criteria (AIC), with preference given to the model with the lowest AIC (Burnham and Anderson, 2004).

Some participants could not reach all of the imposed walking speeds. Therefore, the selection of the best fractional polynomial was performed considering only complete data, and missing data were imputed from the selected fractional polynomial. To include random variability in different strides for each walking speed, a random number was added to the imputed value generated by a normal random variable with mean equal to 0 and variance equal to the observed variance, that is, age group specific between stride variance. The four fitting models converged for walking speeds ranging from 0.3 to 1.1 m/s. Finally, pairwise comparisons among age groups were conducted using Tukey's post hoc test to take into account type I error (alpha). Statistical significance was set at 0.05, two-sided.

Software

Computations, statistics, and creation of graphics were conducted with MATLAB™ (MathWorks Inc., version 8, Natick, MA, USA), SAS version 9.4 (SAS Institute, Cary, NC, USA), and SigmaPlot™ (Systat software Inc., version 10.0, San Jose, CA; USA).

Results

Table 1 presents demographic and anthropometric information for each age group.

Figure 1 shows the 3D path of the CoM for each age group at two distinct ranges of Fr speed, corresponding in this sample to the lowest and the highest Fr reached by all participants. Projections on the three orthogonal planes are also represented.

Between columns, changes in shape with speed are evident. At all ages, the 3D path acquires a more bent, upward concave shape on the frontal plane at the higher (right column) compared with the lower (left column) speed range. Within columns, absolute changes with age are far less evident. The participants' sizes are obviously very different across age groups. In fact, age-related differences emerge if the displacements of the 3D path are standardized to participants' heights, h.

Figure 2 illustrates the relationships between the CoM path parameters and the Fr speed for each age group. The relationships between the CoM path parameters and the Fr speed have a U-shaped curve for each age group. At all speeds, the CoM path parameters are lower, as a rule, as participants get older. In particular, age-dependence holds for the lateral size of the path (x/h) and the total length (path length/h) (top and bottom panels, respectively).

The corresponding fitting equation and the data model fit indices (AIC values) are reported. For each parameter,

Fig. 1

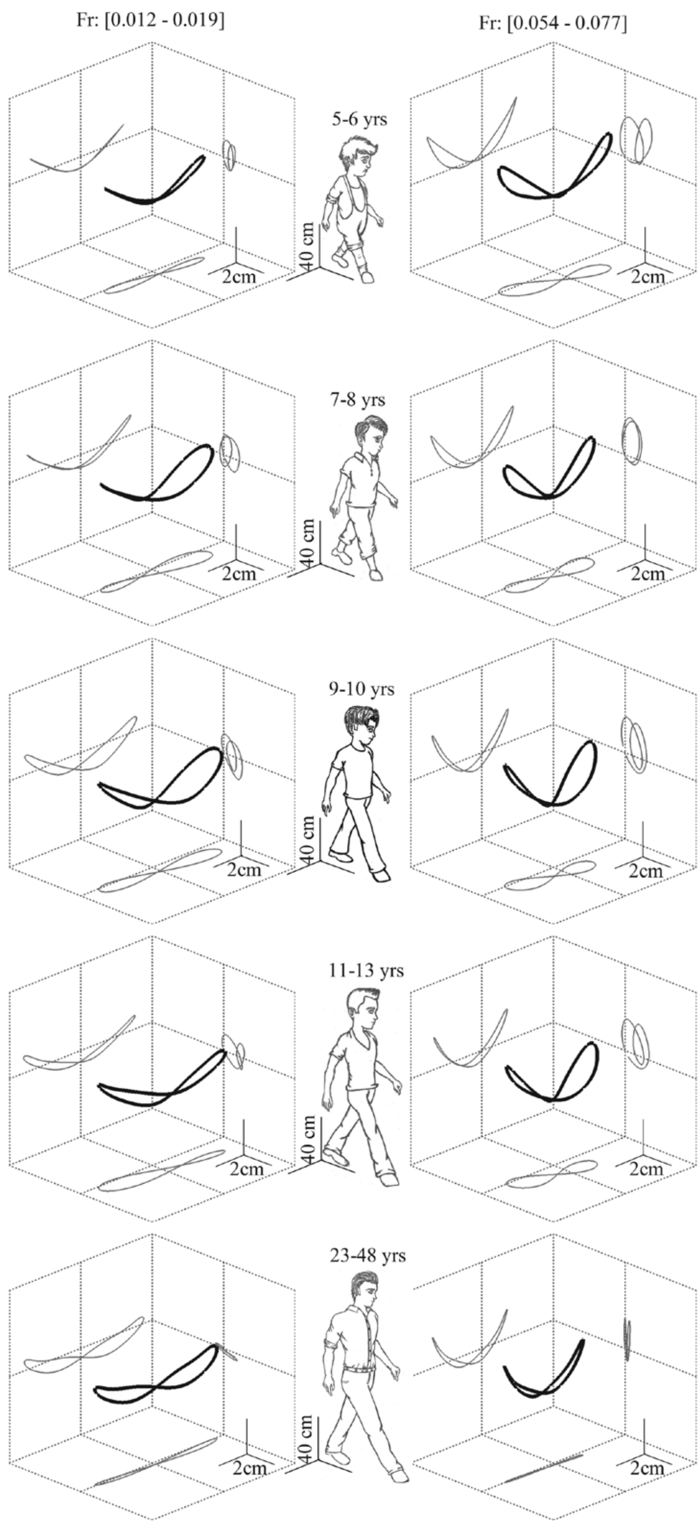

3D path of the CoM during walking on a force-sensing treadmill averaged over six consecutive strides and grand-averaged across participants in each age group. The displacement due to the average forward speed is subtracted. From top to bottom, each panel refers to separate age groups. Each panel represents the mean value of trials obtained for the same range of Froude (Fr) speeds as indicated at the top of each column, that is, 0.012–0.019 Fr (in this sample, corresponding to absolute speeds ranging from 0.38 to 0.56 m/s) and 0.054 to 0.077 Fr (0.90–1.11 m/s). The black and grey curves represent the 3D path of the CoM and its planar projections, respectively. The outline human forms (scaled to the mean participant height across all age groups) highlight the orientation of the spatial coordinates with respect to the walking direction. 3D, three-dimensional; CoM, centre of mass.

Table 1 Characteristics of study participants across age groups

	5–6 years old	7–8 years old	9–10 years old	11–13 years old	23–48 years old
Number of participants	6	6	5	5	6
Sex, male/female	1/5	4/2	3/2	2/3	3/3
Age, years	5.86 (0.35)	7.85 (0.36)	9.61 (0.49)	11.80 (0.74)	32.39 (7.94)
Height, cm	115.88 (4.67)	135.34 (7.86)	143.18 (6.83)	148.49 (6.12)	173.39 (4.61)
Weight, kg	21.48 (3.23)	31.69 (7.37)	41.32 (5.67)	41.71 (6.11)	72.25 (19.63)
Lower limb length, cm	58.60 (3.36)	68.63 (8.86)	75.72 (5.10)	79.37 (4.96)	90.87 (2.81)
ASISd, cm	16.27 (0.57)	17.63 (0.67)	19.82 (0.81)	18.31 (0.87)	25.49 (1.66)

Values for age, height, weight, lower limb length, and ASISd are reported as mean (SD).
ASISd: distance between right and left anterior–superior iliac spines.

the selected second-order fractional polynomial followed this function:

$$Fr^2 + Fr^2 \times \log(Fr) \tag{4}$$

Moreover, for each parameter, the F test associated with the age group covariate had a *P*-value <0.001. Table 2 presents the significance of the 10 possible post hoc contrasts between pairs of age groups. In general, contrasts were only significant between nonadjacent pairs of age groups, and most frequently for the x/h parameter.

In clinical practice, nomograms in which individual parameters can be mapped are needed. Preliminary nomograms of the relationship between the CoM path parameters and the Fr speed are shown in Fig. 3. The 95% confidence limits and 95% individual tolerance (or prediction) limits are also shown.

Discussion

In this study, the 3D path of the CoM during walking was analyzed in healthy children to disentangle effects of age from that of absolute forward speed and body size and to define preliminary pediatric normative values. Few previous studies have investigated the kinematic aspects of the CoM motion such as its 3D path during strides. Therefore, this study is the first to compare the 3D path of the CoM across different stages of child development.

Our results suggest that the CoM path shape changes as a function of speed, mostly in its lateral size, in children 5–13 years of age. A decrease in the lateral oscillation of the CoM with increasing speed has previously been reported in adults walking over normal ground (Orendurff *et al.*, 2004) and on a treadmill (Tesio *et al.*, 2010). Our study adds to this by demonstrating a shrinking of the CoM path laterally with increasing age in children, accounting for the effects of height and absolute speed. In two previous papers, several age-related changes of walking have been described, including the absence of heel strike and push off until after age 2 years, a lack of knee–ankle kinematic coordination in children beginning to walk independently (Forssberg, 1985), and the absence of reciprocal arm swing until the age of a year and a half (Ledebt, 2000). These changes have all been ascribed to the maturation of motor control.

After age 2 years, the pendulum-like energy-saving mechanism of the CoM, a universal characteristic of legged animal locomotion (Cavagna, 2017), appears to be mature (Cavagna *et al.*, 1983). The question of the relevance of age-dependent changes in the CoM trajectory, particularly its lateral size, therefore arises. After all, lateral oscillations of the CoM, following accelerations and displacements of small amplitude, require only a tiny fraction (around 5%) of the total 'external' work needed to keep the body in motion (Cavagna, 1975; Donelan *et al.*, 2004). Our results suggest that balance control rather than energy expenditure is relevant in lateral CoM displacements.

The classic ballistic model of the CoM motion assumes bidimensional (planar) sagittal motion. A clear violation of this model lies in the need for lateral redirection of the 'pendulum' (almost a U-turn) at each step. This happens during the single stance phase, and it requires a weak, yet quick and precise, injection of muscular work against the ground, lasting for 50–100 ms. In this short, yet critical, phase of the step, the curvature of the CoM trajectory peaks and the ballistic efficiency of the pendulum drops to zero giving way to fully active, muscle-driven control (Tesio *et al.*, 2011). This 'turning' phase of the stride has already been highlighted as being at risk for falling sideways even at slow walking speeds (Smeesters *et al.*, 2001) and thus is a target of clinical observation (MacKinnon and Winter, 1993), as it may possibly provide cues to fall prevention (Donelan *et al.*, 2004).

These suggestions were validated in a study in which the dynamic features of the CoM path (its curvature and tangential speed, i.e. its trajectory) were investigated in adults. The study demonstrated that when the CoM has a passive-ballistic, pendulum-like motion, a 'power law' links the tangential speed and the curvature of the CoM (Tesio *et al.*, 2011), like in many other human movements. However, both the ballistic mechanism and its law vanish not only during active forward acceleration (just before and during the double stance) but also when the lateral direction of oscillation is inverted. This suggests that active control is suddenly re-established in these phases of the stride. Notably, the CoM turns actively during mid-stance on a single leg, when the CoM is dangerously moving over the external limits of the supporting foot.

Fig. 2

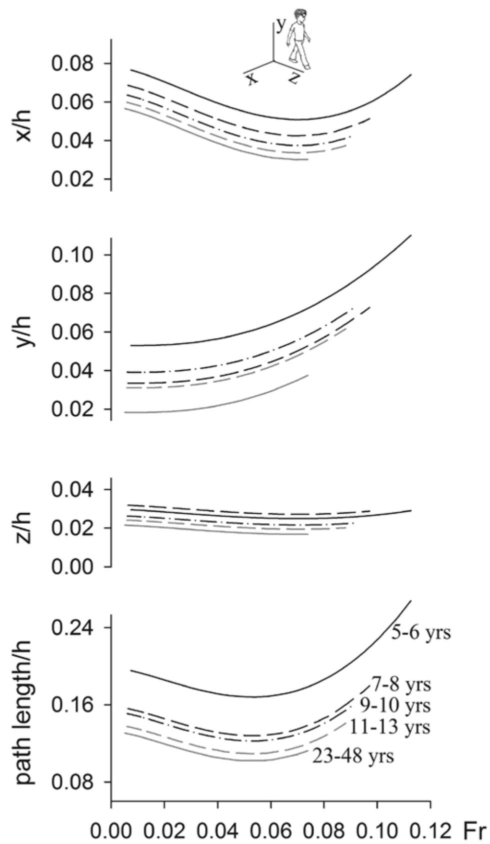

Spatial parameters of the CoM path during one stride on the ordinate, as a function of walking speed (in Froude units, Fr), on the abscissa. From top to bottom, each panel refers to displacements of the CoM, standardized to participant's height (*h*), in the lateral (*x*/*h*), vertical (*y*/*h*), and forward (*z*/*h*) directions, and to the total length of the path (path length/*h*). Note the different scales of path length/*h* with respect to other CoM parameters. Each panel represents the mean value of trials obtained for a range of walking speeds from 0.3 to 1.1 m/s. Curves from the different age groups are superimposed. They can be identified from their distinct tract and from the labels assigned in the bottom panel. The outline human form on the top highlights the orientation of the spatial coordinates with respect to the walking direction. Each of the four parameters of the CoM path was fitted as follows. Subscripts to the group variable refer to the corresponding age group. CoM, centre of mass.

$$x/h = 0.078 + \mathrm{Group}_{23\text{-}48} \times (-0.020) + \mathrm{Group}_{11\text{-}13} \times (-0.017) + \mathrm{Group}_{9\text{-}10} \times (-0.013) + \mathrm{Group}_{7\text{-}8} \times (-0.008) + \mathrm{Fr}^2 \times (23.769) + \mathrm{Fr}^2 \times \ln(\mathrm{Fr}) \times (11.035)$$

$$y/h = 0.053 + \mathrm{Group}_{23\text{-}48} \times (-0.035) + \mathrm{Group}_{11\text{-}13} \times (-0.022) + \mathrm{Group}_{9\text{-}10} \times (-0.014) + \mathrm{Group}_{7\text{-}8} \times (-0.020) + \mathrm{Fr}^2 \times (9.572) + \mathrm{Fr}^2 \times \ln(\mathrm{Fr}) \times (2.328)$$

$$z/h = 0.030 + \mathrm{Group}_{23\text{-}48} \times (-0.008) + \mathrm{Group}_{11\text{-}13} \times (-0.005) + \mathrm{Group}_{9\text{-}10} \times (-0.003) + \mathrm{Group}_{7\text{-}8} \times (0.002) + \mathrm{Fr}^2 \times (4.240) + \mathrm{Fr}^2 \times \ln(\mathrm{Fr}) \times (1.969)$$

$$\text{Path length}/h = 0.199 + \mathrm{Group}_{23\text{-}48} \times (-0.062) + \mathrm{Group}_{11\text{-}13} \times (-0.059) + \mathrm{Group}_{9\text{-}10} \times (-0.046) + \mathrm{Group}_{7\text{-}8} \times (-0.040) + \mathrm{Fr}^2 \times (52.606) + \mathrm{Fr}^2 \times \ln(\mathrm{Fr}) \times (21.587)$$

TABLE 2 Results from the nonlinear regression model for each spatial parameter over Froude (Fr) speed and age group (see Statistics paragraph for details)

Comparison between age groups (years)		*x*/*h*		*y*/*h*		*z*/*h*		Path length/*h*	
		Mean difference (CI 95%)	*P* value	Mean difference (CI 95%)	*P* value	Mean difference (CI 95%)	*P* value	Mean difference (CI 95%)	*P* value
23–48 (*n*=6)	11–13	−0.004 (−0.009–0.001)	0.636	−0.013 (−0.023 to −0.003)	0.104	−0.003 (−0.007–0.002)	0.720	−0.007 (−0.022–0.008)	0.869
	9–10	−0.007 (−0.012 to −0.002)	0.038*	−0.021 (−0.031 to −0.011)	0.001*	−0.005 (−0.009 to −0.001)	0.166	−0.021 (−0.036 to −0.006)	0.057
	7–8	−0.012 (−0.017 to −0.008)	<0.0001*	−0.015 (−0.025 to −0.006)	0.022*	−0.010 (−0.014 to −0.006)	<0.0001*	−0.026 (−0.040 to −0.012)	0.004*
	5–6 (*n*=6)	−0.021 (−0.026 to −0.016)	<0.0001*	−0.035 (−0.044 to −0.025)	<0.0001*	−0.008 (−0.012 to −0.004)	0.002*	−0.066 (−0.081 to −0.051)	<0.0001*
11–13 (*n*=5)	9–10	−0.004 (−0.009 to 0.001)	0.610	−0.008 (−0.019 to 0.002)	0.561	−0.002 (−0.007 to 0.002)	0.869	−0.013 (−0.029 to 0.002)	0.449
	7–8	−0.009 (−0.014 to −0.004)	0.006*	−0.002 (−0.012 to 0.008)	0.990	−0.008 (−0.012 to −0.004)	0.004*	−0.019 (−0.034 to −0.004)	0.106
	5–6	−0.017 (−0.022 to −0.012)	<0.0001*	−0.022 (−0.032 to −0.012)	0.001*	−0.005 (−0.010 to −0.001)	0.096	−0.059 (−0.074 to −0.044)	<0.0001*
9–10 (*n*=5)	7–8	−0.005 (−0.010 to 0.000)	0.270	0.006 (−0.004 to 0.016)	0.806	−0.006 (−0.010 to −0.001)	0.071	−0.005 (−0.020 to 0.010)	0.954
	5–6	−0.013 (−0.019 to −0.008)	<0.0001*	−0.014 (−0.024 to −0.004)	0.064	−0.003 (−0.008 to 0.001)	0.548	−0.046 (−0.061 to −0.030)	<0.0001*
7–8 (*n*=6)	5–6	−0.008 (−0.013 to −0.004)	0.008*	−0.020 (−0.029 to −0.010)	0.001*	0.002 (−0.002 to 0.006)	0.799	−0.040 (−0.055 to −0.026)	<0.0001*
AIC		−8933.8		−7183.6		−8644.8		−7738.6	

The upper row refers to the CoM path parameters, normalized to participants' heights, with lateral (*x*/*h*), vertical (*y*/*h*), and forward (*z*/*h*) displacements and the total length of the 3D path (path length/*h*). The mean difference between age groups and the 95% confidence limits are presented, with *P*-values juxtaposed. The leftmost column presents, in separate cells, the age groups and number of participants (*n*). The next column presents the other three age groups to be contrasted (Tukey's post hoc). Data were obtained for absolute walking speeds ranging from 0.3 to 1.1 m/s.
95% CI, 95% confidence interval; 3D, three-dimensional; AIC, Akaike's information criteria; CoM, centre of mass.
*$P<0.05$

Fig. 3

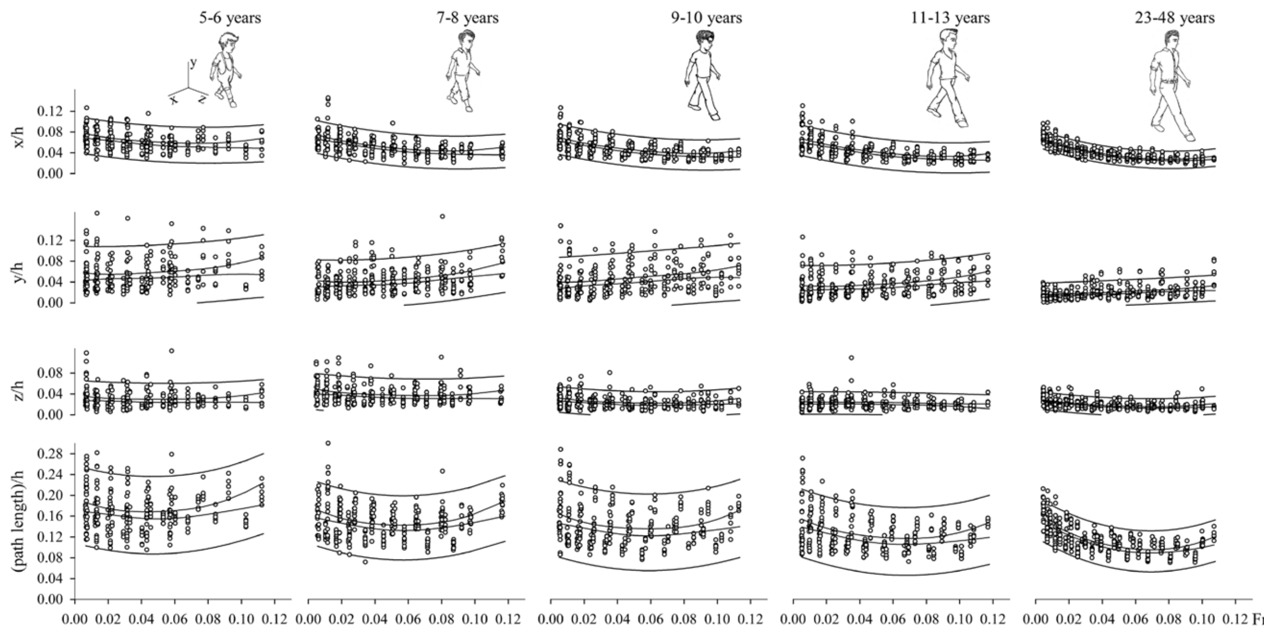

Spatial parameters of the three-dimensional path of the CoM during one stride as a function of walking speed in Froude (Fr) units. From top to bottom, each panel refers to displacements of the CoM in the lateral (***x***), vertical (***y***), and forward (***z***) directions and to the total length of the path, all normalized with respect to participants' heights. From left to right, each column represents different age groups. For all figures, each dot refers to a stride (six strides for each participant). Data were fitted with a second-order polynomial regression equation. Inner and outer continuous lines encase the 95% confidence and tolerance ('prediction') limits, respectively. The lower limits were not represented if negative (thus representing statistical artefacts). The outlined human forms at the top of each column are scaled with respect to the overall mean height and highlight the orientation of the spatial coordinates with respect to walking direction. CoM, centre of mass.

If so, why should the CoM oscillate on the frontal plane, with respect to body size, more in children than in adults at dynamically equivalent speeds? A tentative answer is that the lateral 'shrinking' of the CoM trajectory, relative to body height, reflects the maturation of balance control. This is consistent with the results showing that the absolute width of the base of support is invariant (Thevenon *et al.*, 2015) or even decreasing as age increases (Hallemans *et al.*, 2018). The narrowing of the CoM path therefore makes oscillations over a support base safer as they become relatively narrower with body elongation. This concept is reinforced by results coming from studies directly addressing the spatial relationships between the position of the CoM and the base of support during walking, with special reference to the mediolateral position. In a seminal article (Hof *et al.*, 2005), a vector quantity was defined as the position of the CoM plus its velocity times a factor $(l/g)^{0.5}$, l being leg length and g the gravity acceleration. This quantity was named 'extrapolated CoM', or 'XCoM'. Under dynamic conditions (such as walking), this is the position to be compared in a given direction with the base of support to assess the risk for fall and the need for a timely stepping strategy. The 'margin of stability' was defined as the minimal positive difference between the base of support and the XCoM. In adult walking, the lateral margin of stability is much lower than predicted by considering the CoM alone (about 25 mm vs. 50 mm; Hof *et al.*, 2007). In children, the lateral margin of stability has been found to decrease both in absolute and leg-normalized values. For the 5–11 years age range, close to the age range considered in the present study, this margin decreased from 22 to 12 mm or 4–2% of the leg length, respectively (Hallemans *et al.*, 2018). In short, gait maturation is reflected by the capacity to govern a rather invariant path of the CoM which is travelling closer and closer, with increasing age, to the shrinking lateral margins of stability as defined by the XCoM. In this view, it appears obvious that, despite the modest displacements and the low energetic requirements involved, lateral stability during walking requires considerable motor skill. This largely reflects the development of postural stabilization through anticipatory postural actions (Baldissera and Tesio, 2017). This development appears to begin soon after birth (Girolami *et al.*, 2010). After full myelination of the corticospinal tracts, at around age 5 years, a continuous motor improvement based on implicit learning processes occurs. This is well known for static balance (Cumberworth *et al.*, 2007).

The present study is subject to three important limitations. First, the sample size was small; therefore, it was not possible to consider other potential sources of variability in the statistic model. Second, the age range of participants was limited to within 5 and 13 years, thus preventing a full appraisal of the CoM path along the whole process of development of locomotion. Third, treadmill walking presents some differences with respect to walking over a solid ground. For the same speed, there is a 7–10% shortening of step length. Moreover, at least in children age 6–7 years, a larger step width is observed possibly reflecting difficulties in managing the visuovestibular conflict generated by treadmill walking (Tesio *et al.*, 2017). For these reasons, results can only be generalized with caution. All this considered, it appears acceptable to propose that the motion of the CoM on a treadmill is a promising summary index of the maturation of gait control.

Acknowledgements

This study was funded by the Italian Ministry of Health, "ricerca corrente" 2011, project GAITCORR.

Conflicts of interest

The authors state that they had no interests that might be perceived as posing a conflict or bias in this study.

References

Agostini V, Nascimbeni A, Gaffuri A, Imazio P, Benedetti MG, Knaflitz M (2010). Normative EMG activation patterns of school-age children during gait. *Gait Posture* **32**:285–289.

Alexander RM, Jayes AS (1983) A dynamic similarity hypothesis for the gaits of quadrupedal mammals. *J Zool* **201**:135–152.

Baldissera FG, Tesio L (2017). APAs constraints to voluntary movements: the case for limb movements coupling. *Front Hum Neurosci* **11**:152.

Bennett BC, Abel MF, Wolovick A, Franklin T, Allaire PE, Kerrigan DC (2005). Center of mass movement and energy transfer during walking in children with cerebral palsy. *Arch Phys Med Rehabil* **86**:2189–2194.

Burnham KP, Anderson DR (2004). *Model selection and multimodel inference.* 2nd ed. New York, NY: Springer New York.

Cavagna G (2017). *Physiological aspects of legged terrestrial locomotion: the motor and the machine.* Springer Int Publisher AG Cham, Switzerland

Cavagna GA (1975). Force platforms as ergometers. *J Appl Physiol* **39**:174–179.

Cavagna GA, Franzetti P, Fuchimoto T (1983). The mechanics of walking in children. *J Physiol* **343**:323–339.

Cumberworth VL, Patel NN, Rogers W, Kenyon GS (2007). The maturation of balance in children. *J Laryngol Otol* **121**:449–454.

Cupp T, Oeffinger D, Tylkowski C, Augsburger S (1999). Age-related kinetic changes in normal pediatrics. *J Pediatr Orthop* **19**:475–478.

Dierick F, Lefebvre C, van den Hecke A, Detrembleur C (2004). Development of displacement of centre of mass during independent walking in children. *Dev Med Child Neurol* **46**:533–539.

Donelan JM, Shipman DW, Kram R, Kuo AD (2004). Mechanical and metabolic requirements for active lateral stabilization in human walking. *J Biomech* **37**:827–835.

Forssberg H (1985). Ontogeny of human locomotor control. I. Infant stepping, supported locomotion and transition to independent locomotion. *Exp Brain Res* **57**:480–493.

Girolami GL, Shiratori T, Aruin AS (2010). Anticipatory postural adjustments in children with typical motor development. *Exp Brain Res* **205**: 153–165.

Hallemans A, Verbecque E, Dumas R, Cheze L, Van Hamme A, Robert T (2018). Developmental changes in spatial margin of stability in typically developing children relate to the mechanics of gait. *Gait Posture* **63**:33–38.

Hof AL, Gazendam MG, Sinke WE (2005). The condition for dynamic stability. *J Biomech* **38**:1–8.

Hof AL, van Bockel RM, Schoppen T, Postema K (2007). Control of lateral balance in walking. Experimental findings in normal subjects and above-knee amputees. *Gait Posture* **25**:250–258.

Jensen RK (1989). Changes in segment inertia proportions between 4 and 20 years. *J Biomech* **22**:529–536.

Ledebt A (2000). Changes in arm posture during the early acquisition of walking. *Infant Behav Dev* **23**:79–89.

MacKinnon CD, Winter DA (1993). Control of whole body balance in the frontal plane during human walking. *J Biomech* **26**:633–644.

Moser EB. *Repeated measures modeling with PROC MIXED*. In: *SUGI 29*; 2004. pp. 188–217. SUGI 29 proceedings, Montreal (Canada) 2004. Free download at https://support.sas.com/resources/papers/proceedings/proceedings/sugi29/188-29.pdf

Orendurff MS, Segal AD, Klute GK, Berge JS, Rohr ES, Kadel NJ (2004). The effect of walking speed on center of mass displacement. *J Rehabil Res Dev* **41**:829–834.

Royston P, Ambler G, Sauerbrei W (1999). The use of fractional polynomials to model continuous risk variables in epidemiology. *Int J Epidemiol* **28**: 964–974.

Smeesters C, Hayes WC, McMahon TA (2001). Disturbance type and gait speed affect fall direction and impact location. *J Biomech* **34**:309–317.

Sutherland DH, Olshen R, Cooper L, Woo SL (1980). The development of mature gait. *J Bone Joint Surg Am* **62**:336–353.

Swearingen J, Young J. Determination of centers of gravity of children, sitting and standing. Oklahoma City, OK: Office of Aviation Medicine, Civil Aeromedical Research Institute; 1965. Report AM-65-23.

Tesio L, Lanzi D, Detrembleur C (1998a). The 3-D motion of the centre of gravity of the human body during level walking. I. Normal subjects at low and intermediate walking speeds. *Clin Biomech (Bristol, Avon)* **13**:77–82.

Tesio L, Lanzi D, Detrembleur C (1998b). The 3-D motion of the centre of gravity of the human body during level walking. II. Lower limb amputees. *Clin Biomech (Bristol, Avon)* **13**:83–90.

Tesio L, Malloggi C, Portinaro NM, Catino L, Lovecchio N, Rota V (2017). Gait analysis on force treadmill in children: comparison with results from ground-based force platforms. *Int J Rehabil Res* **40**:315–324.

Tesio L, Rota V, Chessa C, Perucca L (2010). The 3D path of body centre of mass during adult human walking on force treadmill. *J Biomech* **43**: 938–944.

Tesio L, Rota V, Perucca L (2011). The 3D trajectory of the body centre of mass during adult human walking: evidence for a speed-curvature power law. *J Biomech* **44**:732–740.

Thevenon A, Gabrielli F, Lepvrier J, Faupin A, Allart E, Tiffreau V, Wieczorek V (2015). Collection of normative data for spatial and temporal gait parameters in a sample of French children aged between 6 and 12. *Ann Phys Rehabil Med* **58**:139–144.

Virmavirta M, Isolehto J (2014). Determining the location of the body's center of mass for different groups of physically active people. *J Biomech* **47**:1909–1913.